Design of a Robust, High-rate Wireless Sensor Network for Static and Dynamic Structural Monitoring

Matthew J. Whelan and Kerop D. Janoyan

Journal of Intelligent Material Systems and Structures 2009 20: 849 originally published online 28 November 2008
DOI: 10.1177/1045389X08098768

Design of a Robust, High-rate Wireless Sensor Network for Static and Dynamic Structural Monitoring

MATTHEW J. WHELAN[1] AND KEROP D. JANOYAN[2,*]

[1]*Graduate Student, Clarkson University, Dept. of Civil and Environmental Engineering, Potsdam, NY 13699-5712*

[2]*Associate Professor, Clarkson University, Dept. of Civil and Environmental Engineering, Potsdam, NY 13699-5710*

ABSTRACT: Over recent years, there has been much interest in the use of low-cost wireless transceivers for communication of sensor data to alleviate the expense of widely distributed cable-based sensors in structural monitoring systems. However, while the number of unique wireless sensor platforms has continued to expand rapidly, the lack of success in replicating the number of deployed sensors and sampling rates utilized in previous cable-based systems has led to disillusionment over their use for this application. This article presents a wireless sensing system designed for concurrent measurement of both static and dynamic structural response through strain transducers, accelerometers, and temperature sensors. The network protocol developed supports real-time, high-rate data acquisition from large wireless sensor arrays with essentially no data loss. The current network software enables high-rate acquisition of up to 40 channels across 20 wireless units on a single peer-to-peer network with system expansion enabled through additional networks operating simultaneously on adjacent communication channels. Elements of the system design have been specifically tailored towards addressing condition assessment of highway bridges through strain-based load ratings as well as vibration-based dynamic analysis. However, the flexible system architecture enables the system to serve essentially as an off-the-shelf solution for a wide array of wireless sensing tasks. The wireless sensing units and network performance have been validated through laboratory tests as well as dense large-scale field deployments on an in-service highway bridge.

Key Words: structural health monitoring, wireless sensor networks, vibration monitoring, load rating, bridge inspection.

INTRODUCTION

As a significant portion of the aging network of highway bridges have met or exceeded their intended design lifetime and service limits, highway administrations are faced with the challenging task of allocating limited resources for replacement and rehabilitation of the structures most critical for repair while managing the remaining end-of-life bridges without jeopardizing public safety. As demonstrated in the aftermath of recent bridge collapses over the past several decades, current schedule-based visual inspections fall short of ensuring a safe operational model for highway bridge management with bridge closures preceding imminent failure. Visual inspections introduce significant subjectivity and variability as evidenced by Moore et al. (2001) in a study conducted for the Federal Highway Administration (FHWA). In this study primary members individually inspected by a group of inspectors were assigned, on average, four to five different ratings on the scale of 0–9. It was found that inspectors were hesitant to assign condition ratings outside of the mid-range ratings, often lacked a 'formulated, systematic approach' in assigning condition ratings, and were unlikely to detect localized defects, such as weld crack initiations. Visual inspections simply lack the ability to identify deterioration that is inaccessible or is simply invisible to the inspector. Overloading, settlement, fatigue damage, and locked bearings can often only be visually identified in the most extreme cases. Furthermore, the FHWA acknowledges that assessment ratings provided in the National Bridge Inventory (NBI) by visual inspections do not provide adequate detail for managing maintenance programs and planning rehabilitations (Chase, 2005). Even basic operational data such as traffic counts, operational service demands, and truck weights are unknown, thereby impeding quantitative cost-benefit analysis in determining allocation of resources.

Structural monitoring through sensor technology to characterize deterioration of bridge components, in order to evaluate safety and advise repair in advance of failure, has long been proposed (Kato and Shimada, 1986).

*Author to whom correspondence should be addressed.
E-mail: kerop@clarkson.edu

1045-389X/09/07 0849–15 $10.00/0 DOI: 10.1177/1045389X08098768

In general, approaches either prescribe installation of instrumentation on the bridge for continuous monitoring throughout the service life of the bridge or enhance periodic, schedule-based inspections through the incorporation of quantitative sensor data. Currently, even the low-power wireless sensors are limited in terms of duration of unattended deployment, due to the limited capacity of battery power supplies. As a consequence of the number of highway bridges in need of in-service assessment and the obstacles to continuous monitoring, it is likely that wireless sensors will be foremost used to accompany inspection routines for periodic condition assessment, with long-term monitoring reserved only for critical structures having significant investment in terms of cost and potential for high loss of life.

Transmitting data using a wireless transceiver presents several obstacles to distributed sensing, particularly limited and shared transmission bandwidth, coordination of decentralized hardware, and the possibility that the data packets will be dropped due to radio frequency signal corruption. A review of recent wireless sensor deployments for structural health monitoring of bridges (Table 1) reveals that the networks have generally relied upon one of either two approaches: (1) low sampling rates and/or limited numbers of sensors to achieve real-time transmission, or (2) local data logging and post-sampling transmission of sensor data. Reduced sampling rates may be acceptable for some bridges where there are many low natural frequencies; however moderately stiff and stiff bridges, such as integral abutment and short-span bridges, necessitate higher sampling rates as well as large number of sensors to capture and spatially resolve a sufficient number of modes for analysis. For short-term monitoring, data logging may be an acceptable approach to ease the burden on the transceiver bandwidth limitation; however this architecture eliminates the possibility of sampling histories beyond several minutes and generally necessitates a much longer time period to recover the data across the wireless link. Furthermore, the additional time required for post-transmission of sampled data mandates a significant increase in the duration of time that the microcontroller and, in particular, the radio transceiver must be active and drawing power from limited battery resources. For instance, a recent deployment using a data logging and post-sampling approach required 9 h to transmit a total of 20MB of network data following onboard sampling for an effective average transmission bandwidth of ~0.6 kbps (Pakzad et al., 2008). This additional active time ultimately restricted the network deployment to 13 data sets before the relatively large power reserve, which consisted of four 6 V lantern batteries at each node or 180 Whr, was exhausted. In contrast, the current study maintained an effective network bandwidth of over 100 kbps while concurrently handling sampling tasks, thereby marking an improvement in several orders of magnitude in terms of network bandwidth, effective sampling duration, and, ultimately, power consumption.

Other studies have suggested that onboard data processing to alleviate bandwidth limitations and reduce power consumption should be pursued in favor of transmission of complete time histories (Lynch et al. 2004). However, without complete time histories the analysis is restricted to the onboard computational analysis, thereby eliminating the possibility of employing several analysis or damage detection algorithms to the data. This approach also prohibits the development of a database of sensor measurements for complementary data mining, i.e., for extraction of operational information related to traffic counts, stress cycles, and service demands. In short, utilizing wireless sensor networks as an alternative to cable-based instrumentation systems should not be accompanied by excessive concessions in terms of performance and data extraction. The system described in this article has achieved the higher sampling rates required while maintaining reliable communication of time histories within a large, dense array of sensors, effectively replicating previous cable-based structural health monitoring test programs.

Table 1. Survey of wireless bridge monitoring field deployments.

Deployment	Network description	Data delivery	No. of sensors	Sampling rate
Pakzad et al. (2008)	64 nodes log data from two channels over a sampling time of 1600s. Data is streamed after sampling resulting in a significantly more time consuming stage (9 hours total).	Post-sample delivery of logged data	128 Accel.	50 Hz
Paek et al. (2006)	Five local networks of 4 nodes each with a single-board computer base station connected to an IEEE802.11b wireless radio.	Real-time	20 Tri-axis Accel. (4 per network)	20 Hz
Lynch et al. (2006)	A wireless sensor network on a concrete box girder bridge alongside a wired system.	Real-time	14 Accel.	70 Hz
Current study	A dense, multi-sensor wireless network on a single-span concrete deck on steel girder bridge.	Real-time	40 Channels, mixed Accel/Strain	128 Hz

HARDWARE DESIGN

The Wireless Sensor Solution (WSS) developed within the Laboratory for Intelligent Infrastructure and Transportation Technologies (LIITT) at Clarkson University was designed as a universal platform for high-rate, large-scale monitoring of structural response (Figure 1). The sensor network is composed of an array of distributed sensing nodes that interface with sensors, condition analog signals, then convert them to digital format and transmit the readings to a base coordinator. The base coordinator features the same wireless transceiver hardware as the remote nodes; however, its function is to control bi-directional wireless communications between the host computer and the distributed sensing units. The base coordinator is connected to the host computer across a Universal Serial Bus (USB) connection as a virtual COM device. This physical hardware interface is advantageous as it enables either network control from a CPU local to the measurement site or remote access across an internet connection through TCP/IP protocol using a network-enabled USB hub. The primary hardware issues addressed in design of the wireless sensing units were appropriate signal conditioning for the range of responses typical of the spectrum of highway bridge designs and span-lengths, minimized power consumption for battery resource conservation, and high-throughput network communications.

Wireless Sensor Network Platform

A wireless sensor node is comprised of a traditional sensor, appropriate signal conditioning hardware, and a transceiver platform for onboard processing, control, and communications. The advent of low-cost radio-frequency chip transceivers has led to the development of a significant number of commercial wireless sensor network platforms with various microcontroller and transceiver chip combinations, each with certain advantages and disadvantages relative to the sensor application (Lynch and Loh, 2006). Processor speed, onboard memory, analog-to-digital converter (ADC) specifications, digital I/O port access, power consumption, communication range, transceiver data throughput, and host communication bus throughput must all be considered in the selection of an optimal wireless sensor network platform for any application.

Figure 1. *WSS node with accelerometer and strain transducer.*

The developed wireless sensor node (Figure 1) incorporates the Tmote Sky wireless sensor network platform developed by researchers at the University of California at Berkeley and marketed by the MoteIV Corporation. This platform integrates an ultra-low power microcontroller and chip transceiver on a single printed circuit board with a USB interface to the host computer for microcontroller programming and communication. The onboard Chipcon CC2420 2.4 GHz transceiver offers an effective data rate of 250 kbps, enabling real-time packet transfer from high-sampling rate deployments. The transceiver is a spread spectrum modem, which provides substantial resilience to the interference relative to narrow-band communication modems; this is vital for reliable communication in the increasingly noisy 2.4 GHz frequency band. The printed circuit invert-F antenna on the Tmote Sky enables an approximate communication range of 50 m indoors and 125 m outdoors, while an external antenna can be used to extend the range beyond 500 m (Whelan et al., 2008). As previously mentioned, low power consumption is imperative for long-duration wireless deployments as the system life is dictated by the power supply resources. The CC2420 chip transceiver features one of the lowest current consumption specifications of the IEEE802.15.4 family of modems; the receiving state consumes 18.8 mA, the transmission state consumes 17.4 mA at 0 dBm output power, and three ultra-low idle modes reduce consumption to as low as $<1\,\mu A$. The Tmote Sky hardware is compliant with US and Canadian radio frequency regulations and is certified by the Federal Communications Commission (FCC) and Industry Canada for unlicensed use in either country.

The Texas Instruments MSP430F1611 ultra-low-power microcontroller provides the computational core of the Tmote Sky platform. This 16-bit microcontroller has 48 kB of flash memory for embedded code storage as well as 10 kB of RAM. When running at 1 MHz at a supply voltage of 3 V, the microcontroller consumes a nominal 500 μA of current; low-power modes can reduce the consumption to $<1\,\mu A$. An integrated 12-bit successive approximation register (SAR) ADC provides eight external channels and greater than 200 ksps maximum conversion rate. Conversions are triggered by a timer sourced from a clock oscillator for accurate, hardware-timed sampling rates. Two universal synchronous/asynchronous serial communication buses are available for four-wire serial peripheral interface (SPI),

two-wire serial (I2C), or universal asynchronous receiver/transmitter bus protocol. Dual communication buses permit the microcontroller to transmit data between the radio and the host computer at the base coordinator without sharing communication lines, so as to maintain high throughput. Other notable peripherals include a two-channel digital-to-analog converter (DAC), a three-channel direct memory access (DMA) controller for high-speed data transfers, a hardware multiplier for efficient computations and onboard data processing, two 16-bit timers with interrupt capability, and a watchdog timer for automated system recovery in the event the software hangs.

Sensor Interface and Signal Conditioning

The WSS hardware features a low-power signal conditioning board that improves the quality of the analog sensor signals relative to the ADC range and sampling parameters prior to digital conversion. The conditioning interfaces were designed to be optimized for measurement of vibrations resulting from both ambient and forced excitation as well as acquisition of strain transducer outputs during typical load ratings. However, whenever possible, integrated circuits with a wide range of reprogrammable features were selected to maintain the flexibility for additional sensing applications outside of bridge monitoring. The sensor nodes are multi-functional in that they accommodate acquisition of up to two signal-conditioned single-ended voltage signals, a differential analog sensor signal, and up to three resistive or diode-based sensors, such as thermistors or thermodiodes for temperature measurement.

SINGLE-ENDED ANALOG SIGNAL CONDITIONING

To facilitate high-resolution acquisition of distributed acceleration measurements for modal analysis of structures, a custom signal conditioning sub-circuit provides analog low-pass filtering, digital offset correction, and digitally programmable gain for up to two single-ended analog signals. A 3 V voltage reference sources ultra-low noise, stable power to the sensors, and filter operational amplifiers. Providing a regulated supply to the sensors reduces output noise as well as maintaining the sensitivity to enable conversion from voltage to acceleration using a single calibration constant. The analog filters enforce a Butterworth frequency response with a 100 Hz frequency bandwidth (-3 dB) and are provided to prevent aliasing of higher frequency signal components. Each filter is a fifth-order Sallen-Key circuit design featuring dual second-order sections on the signal conditioning board with the real-pole provided at the external accelerometer. Placement of the real-pole filter with the accompanying buffer amplifier enables greater noise immunity through low-impedance output at the signal source and permits the connection of other MEMS accelerometers, which generally have different internal resistance on the signal output path. The low-noise, low-power Linear Technologies LT6915 programmable gain amplifier (PGA) was selected to maximize the resolution of the conversion specific to the signal input range or on-site vibration amplitude. In-network commands enable remote programming of 14 gain settings available in binary multiples. Independent non-volatile programmable voltage references set through the use of the microcontroller 12-bit DAC are used to digitally correct signal offsets, such as the gravitational offset of each accelerometer, prior to amplification. Signal offset nulling adjusts the signal input range such that it is balanced in both the positive and negative directions, and permits the use of higher gain amplification without driving the signal out of range. An embedded software algorithm performs this adjustment automatically to enable rapid configuration of the sensors with a single network command. The PGA output is biased with a 1.25 V reference, which is the mid-span of the ADC conversion range that is set with an external 2.5 V reference. Hardware shutdown of the PGA, voltage reference supply, filter sections, and sensor excitation conserves limited battery resources during periods of inactivity.

DIFFERENTIAL ANALOG SIGNAL CONDITIONING

An independent signal conditioning interface is provided for the acquisition of differential sensor signals, such as Wheatstone-bridge resistive sensors like strain transducers, load cells, pressure sensors, and displacement sensors. To perform a strain-based load rating, a large array of strain transducers are required for measurement of the induced strains and strain profiles to known loads, for calculation of neutral axis locations, distribution factors, end fixity, and impact factors to derive an overall rated load capacity of the bridge. An application-specific integrated circuit (ASIC) was incorporated into the design, which condenses the signal conditioning and acquisition hardware for differential signal and full-bridge resistive sensors into a single integrated circuit. The ZMD31050 Advanced Differential Sensor Signal Conditioner features 13 stages of programmable gain of up to 420 V/V, digitally programmable analog offset nulling, and a 15-bit internal ADC with adjustable input range. Additionally, an input channel is provided for temperature measurement using a thermistor in a half-bridge configuration. An internal calibration microcontroller introduces a digital conditioning algorithm for up to third-order correction of sensor nonlinearity as well as providing temperature compensation using the external thermistor. Temperature compensation is a critical correction for long duration strain measurements using

strain transducers, as the temperature-induced expansion of bridge elements often differs with temperature-induced transducer expansion, thereby resulting in a strain output in the absence of applied deck load that is an incorrect measure of temperature-induced strain. Another advantageous feature for long-term monitoring is the novel error detection hardware embedded in the ASIC for automatically sensing damaged sensors or broken cabling; two comparators monitor the input voltages, and the output register is set to an error code in the event of a broken wire. The ASIC communicates with the MSP430 microcontroller across the I2C communication bus, which is used to program the signal conditioning hardware and acquire readings from the ADC. A conditioned analog output is also wired to the microcontroller ADC to enable higher rate acquisitions concurrently with the single-ended sensor circuits. Power conservation is addressed similarly to the single-ended signal conditioning circuitry, with digitally controlled hardware shutdown of the 3 V voltage regulator used to supply low-noise, regulated power to the transducer and ASIC.

WSS SOFTWARE DESIGN

Software was designed specifically for the wireless sensor nodes to utilize the advantageous hardware features selected and incorporated in the design. The integration of advanced hardware peripherals with optimized software algorithms is directly responsible for the large-scale high-rate wireless sensor network operation achieved in field testing that has exceeded the performance characteristics of concurrent wireless structural health monitoring platforms. Software for the WSS system encompasses both embedded software for the remote and central coordinator nodes, as well as PC software for bi-directional communication with the central coordinator nodes, real-time display, and data logging.

Embedded Software

The embedded software applications for both the remote and coordinator nodes were written in C code, compiled, and programmed under the loose framework of the TinyOS-1.x open-source operating system. While the TinyOS project and the accompanying assembler code were utilized for programming the motes, the software modules and interfaces were generally found to be insufficient for meeting the requirements of large-scale, high-rate structural health monitoring and were therefore seldom used. Extensive development of low-level software to incorporate the advanced hardware peripherals resulted in significantly increased data throughput, with a greater number of nodes per network while maintaining reliable transmission. For instance, the introduction of direct hardware interrupt-driven handling of certain microcontroller events, in contrast to first-in-first-out (FIFO) handling of software events, allowed for prioritization of certain critically timed tasks. For instance, hardware interrupt handling of the completion of analog-to-digital conversions permitted the alleviation of software delays resulting in memory overflow of the ADC buffer and the associated temporal sampling jitter. Software development also enabled the introduction of digital signal processing of the sensor measurements, specifically through the use of the microcontroller hardware multiplier for digital low-pass filtering.

The embedded software was designed to balance efficiency and throughput with flexibility, so that the same code could be utilized for an array of monitoring tasks and sensor network configurations. A set of in-network radio messages, identified by a single-byte ID, are handled by the embedded software to perform configuration and status return tasks as well as initiate sampling routines. The software allows in-network selection of node independent sensor channels, sampling rates, and monitoring durations. Configuration of the signal conditioning circuitry is also handled by the embedded software in response to node independent messages from the coordinator. The PGA gain setting for each single-ended channel is user-selected through the PC host software. Upon reception of the configuration message for the single-ended signal conditioning circuit, the embedded software measures the offset of each channel, nulls the offsets to the mid-span of the ADC input range using programmable voltage references, and establishes the signal gains using a digital output to a 4-bit binary counter interfaced with the parallel inputs of the PGA. Automatic offset correction and programmable gain facilitate rapid sensor deployment and alleviate the burden of physical user interaction and knowledge of the underlying hardware. Configuration of the differential signal conditioner for the strain transducer is handled similarly, though the user is provided full access to the memory registers of the ASIC through the PC host software. Following programming of the ASIC, the signal offset of the conditioned differential signal is measured and an optional iterative scheme is applied through the embedded software, to adjust the extended analog offset compensation register until the signal is within achievable tolerance of the mid-span of the output range. Commands from the central coordinator node also trigger queries of configuration settings, establish sub-circuit power supply operation, and initiate low-power sleep periods. The query response is displayed on the PC host software to indicate the status of the wireless nodes, battery voltage, configuration settings, temperature readings, and received signal strength

indication (RSSI) for providing a measure of the RF transmission power.

SAMPLING ARCHITECTURE

An over-sampling approach is implemented within the embedded software during the acquisition of measurements from the MSP430 12-bit ADC, in order to increase the effective resolution of the conversion as well as to virtually eliminate signal attenuation in the measured bandwidth. Sensor data is over-sampled and then passed through a digital low-pass filter prior to down-sampling to the desired effective data rate that is transmitted across the radio. The digital filter is implemented by the embedded software with the microcontroller hardware multiplier; coefficients and decimation ratio can be remotely programmed to override defaults. The use of over-sampling reduces the effect of ADC quantization noise and is generally accepted to provide an additional bit of effective resolution for each power of four rate of over-sampling.

A default digital low-pass filter and decimation rate stored in the microcontroller memory have been established to maximize the non-attenuated bandwidth of the measured signal while producing sufficient attenuation of frequency components passed by the analog low-pass filter (Figure 2). A 56th-order finite-impulse response (FIR) digital filter of the Equi-Ripple design has been implemented with a specified maximum ripple of 0.01 dB in the pass-band and a minimum attenuation of 52 dB in the cut-off. At a sampling rate of 128 Hz, the pass-band encompasses 0–50 Hz and the cut-off frequency of the filter is 78 Hz. This design allows frequency components from 64–78 Hz to alias into the 50–64 Hz bandwidth in order to maximize the non-attenuated measurement bandwidth. The cut-off frequency of the analog filter was deliberately set higher than the anticipated measurement bandwidth due to the relatively poor roll-off characteristics of the analog filter. The filtering approach taken also affords greater flexibility of the measurement bandwidth relative to an analog-only filtering design as the digital filter and sampling rate can be reprogrammed to enable any desired measurement bandwidth up to the 100 Hz cut-off of the analog hardware filter.

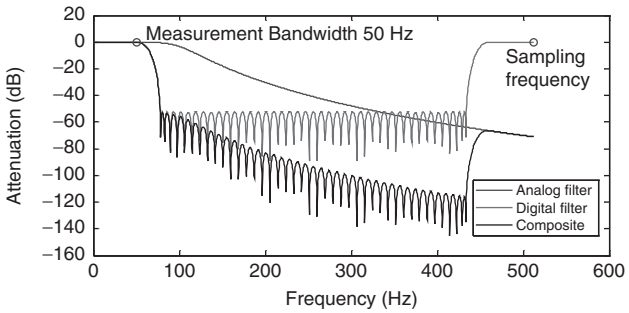

Figure 2. *Anti-aliasing filter response.*

RADIO TRANSMISSION PROTOCOL

In order for wireless sensors to serve as an effective alternative to cable-based instrumentation for bridge monitoring tasks, the network capabilities must at least permit replication of the number of sensors as well as the sampling rates utilized in typical cable-based deployments. The use of a bi-directional, adaptive, and coordinated radio transmission protocol to govern network communications is essential for reliable data reception in a large sensor array operating with high data throughput. The protocol developed, displayed schematically in Figure 3, has been found to support up to 40 channels of sensor data with per-channel sampling rates of up to 128 sps in a single network. Furthermore, data completion rates in field tests have validated that the protocol yields virtually 100% packet delivery. This system-level performance signals that the use of wireless sensor networks for structural health monitoring has emerged as a currently technologically feasible approach.

Scheduling of packet transmissions was found to be essential to prevent significant packet loss from collisions when maintaining concurrent communication among a high volume of deployed sensor nodes. The protocol implemented assigns a sequential time offset between transmissions based on the local address of the node. However, sampling initiation is not offset amongst the nodes in the network; all nodes initiate sampling simultaneously as triggered by a single command from the central coordinator node. Transmission scheduling is integrated into the ADC sampling routine so that the protocol is adaptive to sampling frequency. The nodes utilize the FIFO transmission buffer in the CC2420 transceiver to temporarily hold the packet to be transmitted until the time window scheduled for transmission occurs. To additionally guard against loss of data due to packet collision, the clear channel assessment (CCA) feature of the chip transceiver is utilized, whereby the packet is only transmitted if the measured RSSI is below the specified threshold value and no IEEE802.15.4 data is being transmitted across the current channel.

Despite local transceiver scheduling, there is no guarantee that transmissions will be received by the central coordinator and without bit errors. However, providing nodes with an indication of successful packet reception through bi-directional communication allows the embedded software to determine whether to schedule the packet for retransmission. All data packets request an automatic acknowledgement packet from the central coordinator, which is returned only in the event that the packet is received and passes a cyclic-redundancy check (CRC) for bit errors. The transmission schedule

developed provides an additional time slot for retransmission of packets failing to receive an acknowledgement of host reception. In the event that the retransmission also fails to receive an acknowledgement, the complete data packet is transferred to a transmission queue for retransmission during available radio access time. These instants of availability occur during the local node-scheduled time for retransmission of packets failing to receive acknowledgement on the first attempt, if the previous packet was successfully acknowledged, or at the conclusion of the data sampling. During system validation, the transmission queue rarely contained more than a few packets and any packets transmitted at the conclusion of sampling were generally from the final seconds of the sampling duration. A watchdog timer is also implemented during the sampling and radio transmission routine, to recover the system in case the embedded software become unresponsive during this period of high overhead for the microcontroller.

TIME SYNCHRONIZATION

Since all nodes are independent hardware devices, they each operate with their own clocks that will have unique offset and drift characteristics that affect the relative timing of tasks among all nodes in the network. As system identification algorithms often require synchronous sampling of sensor signals and the network radio protocol developed relies on coordination of the individual nodes, simultaneous initiation and time synchronization of the remote WSS nodes was addressed in the software design. The CC2420 transceiver allows packets to be addressed either to specific nodes or to be broadcast to all nodes in the network. The use of a generic message to initiate sampling across the entire network with a broadcast packet enables the initiation of sampling across all nodes at nearly the same instant. Deviations in sampling initiation time arise from the RF propagation duration and deviations in processor clock frequencies when handling the sampling initiation packet and preparing the hardware for sampling. Given that electromagnetic waves propagate at the speed of light (Griffiths, 2006), the time of reception deviation between nodes with a 100 m difference in their distance to the central coordinator will be on the order of nanoseconds and therefore introduce virtually no phase error for the sampling

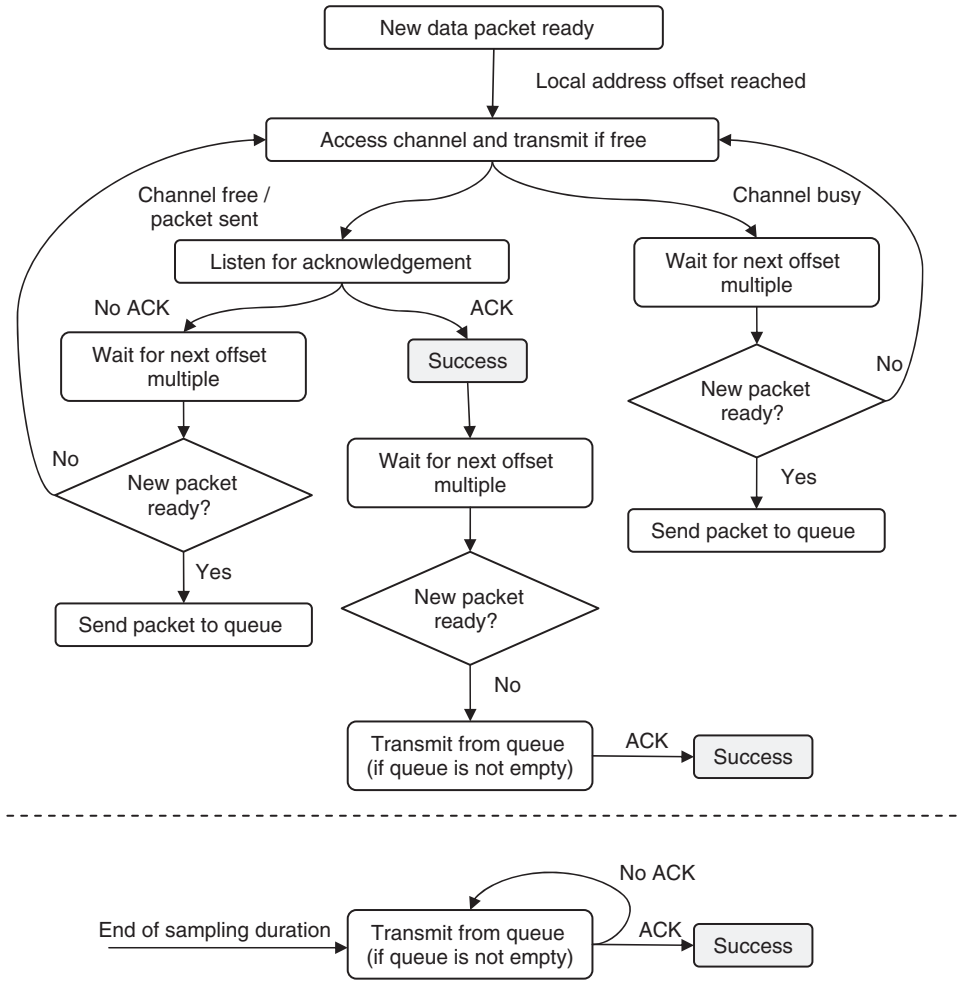

Figure 3. *Radio transmission protocol flow chart.*

periods used, which are on the order of milliseconds. Since the main clock is sourced by a 4 MHz digitally controlled oscillator (DCO), phase differences in the clocks affecting the interrupt handling of the sampling initiation packet from the chip transceiver are also on the order of nanoseconds. To ease any time delay introduced through handling the sampling initiation routine, the signal conditioning and ADC/Timer register configuration is handled by a separate message. Since this reduces the initiation of sampling to only a few instructions, any variability in DCO frequency across the network should result in negligible offset in sampling initiation. Consequently, the predominant source of any initial phase error in the sampling timers is derived from any phase difference among the sample-and-hold source clock for the ADC. The 32 kHz crystal oscillator source currently utilized contributes a maximum 30 μs difference in sampling initiation.

Maintaining a stable, accurate timer source for the ADC is imperative in order to produce accurate measurement of modal frequencies and extract mode shapes, as well as to prevent clock drift from affecting the radio transmission protocol. Main clocks integrated in microcontrollers, such as the internal DCO of the MSP430F1611, generally exhibit poor stability in regard to supply voltage and temperature. The MSP430F1611 is specified with a nominal supply voltage drift of 10% per volt with a temperature drift of +/−0.1% per degree Celsius. While the WSS nodes are equipped with voltage regulators supplying the microcontroller voltage, which eliminates supply voltage-induced frequency deviation, the initial accuracy of the DCO is generally unacceptable for maintaining time synchronization across the network over any length of time. As an alternative, a 32.768 kHz crystal oscillator is used as the sample-and-hold source clock to trigger ADC conversions.

The 32.768 kHz crystal oscillator incorporated into the Tmote Sky design has a frequency tolerance of +/−20 ppm at 25°C. Assuming a worst-case scenario in which the maximum difference in crystal frequency among sequential nodes in radio transmission protocol is 40 ppm, or 1.3 Hz, the transmission protocol will maintain the prescribed transmission schedule over a minimum sampling duration of 3 min and 15 s for an effective sampling rate of 128 Sps. Laboratory investigation of long-term performance of the radio transmission protocol has confirmed that packet transmission from select nodes in a twenty-node network is generally impaired after 4 or 5 min of continuous sampling when utilizing the 32.768 kHz crystal to trigger ADC samples. Fortunately, 3 min sampling intervals provide more than sufficient frequency resolution for modal analysis and are consistent with previous cable-based studies (Wenzel and Pichler, 2005). In order to enable longer duration sampling and address issues associated with additional temperature-induced clock drift, a packaged temperature-compensated real-time clock can be introduced to the hardware at the expense of slightly increased power consumption. Alternatively, the number of sensor nodes per network can be reduced to increase the continuous sampling duration.

CENTRAL COORDINATOR SOFTWARE

The embedded software operating on the central coordinator node provides the means for bridging the wireless sensor network to a host computer. Interrupt-driven routines provide a transparent interface between the CC2420 transmission and reception buffers and the virtual serial COM port operating at 262,144 baud over a USB connection. Priority is given to transfer of received wireless packets to the host computer in order to prevent overflow of the 128-byte reception buffer in the transceiver. In the event of reception overflow, the microcontroller transfers any complete packets remaining in the buffer and then flushes it to resume normal transceiver operation.

To enable deployment of a high-density wireless sensor network, frequency division multiple access (FDMA) has been implemented to enable multiple 20-node networks to operate simultaneously on different frequency channels. During programming, nodes are assigned a group identification and default communication frequency. In-network commands can reassign a group to another frequency channel in the event of interference from other 2.4 GHz devices. The IEEE802.15.4 standard specifies 16 channels within the legal bandwidth in the US from 2405 MHz to 2480 MHz, thereby enabling concurrent deployment of up to 320 sensor nodes across 16 networks. To maintain time synchronization among multiple networks, a common external switch supplies an interrupt signal to all central coordinators for simultaneous transmission of the sampling initiation command.

PC Host Software

A high-level LabVIEW host PC application has been written to operate in conjunction with the remote transceivers to control and coordinate the wireless networks. User-friendly interfaces permit in-network adjustment of sampling parameters and sub-circuit configurations of the sensor nodes through the extensive in-network command library, supported by the developed embedded software and documented previously in this article. The PC host software enables independent configuration of nodes in the network, as configuration messages are addressed to specific local addresses. Additionally, the host software permits the configurations to be specified with on-screen toggles and menu rings to reduce the in-network programming of these individual configurations to triggering by a single

on-screen button, rather than requiring the user to sequentially send commands to each node. This facilitates the rapid deployment of functionally diverse nodes performing only the tasks specific to the current monitoring program and sensor layout. An extensive digital filter design sub-section of the host software allows the operator to design a custom filter, the coefficients of which can be wirelessly transmitted to the nodes for implementation in the sampling routine. The response to network status queries are reported on-screen to allow indication of the network status, state of the component power supplies, regulated mote supply voltage for indication of low battery resources, temperature readings, and received signal strength. The status query response also includes the programmed offset correction of the accelerometer signal for indication of the sensor orientation relative to the gravitational field. Upon initiation of sensor sampling, the host software receives incoming data packets, displays the measurements in real-time on a waveform chart, and logs the readings to individual spreadsheet files for post-processing.

WSS PROTOTYPE

Prototype sensor nodes were assembled in-house using printed circuit boards commercially manufactured from the board layout design (Figure 4). The printed circuit boards and battery supply are housed in a weatherproof enclosure to ruggedize the nodes for deployment on the exterior of structures. Sensor connectors are watertight IP68 compliant PCB-mount connectors with o-rings to maintain the integrity of the enclosure. An external switch with an o-ring seal is provided to easily cycle power to the node without opening the enclosure. The use of the inverted-F antenna printed on the Tmote Sky circuit board eliminates the need to mount an external antenna through the weatherproof enclosure. The exterior dimensions of the wireless sensor node are 12 cm × 6 cm × 6 cm.

Power Consumption

Power consumption was weighted heavily in the design of the circuitry and selection of integrated circuits since the service life and/or duty cycle of the wireless sensor unit will be dependent on the capacity of the batteries or dictated by the generally low power delivered by power harvesting alternatives. Digitally controlled shutdown of devices through internal low-power modes or hardware switching of supply voltage lines is consequently a critical consideration in component selection and circuit design for wireless sensor nodes. The approximate power consumption of a WSS sensor node based on device specifications and verified with laboratory measurements is itemized in Table 2. Active power draw refers to the power consumption while the node is providing excitation to sensors, actively conditioning the outputs, converting the analog signals to digital format, and transmitting the data across the radio. During periods of idle node

Table 2. Approximate power consumption of wireless sensor node (*-revision).

	Active power	Low power	Low power*
CC2420 transceiver	59.4 mW	0.07 μW	0.07 μW
MSP430F1611 microcontroller	2.5 mW	10 μW	10 μW
Non-utilized Tmote sky devices	36 μW	36 μW	36 μW
Main voltage regulator	0.56 mW	0.56 mW	–
ADC voltage reference	0.25 mW	0.25 mW	–
LTC6915 PGA	2.9 mW (×2)	3.3 μW (×2)	3.3 μW (×2)
Analog filters	1.55 mW (×2)	–	–
Voltage references (single-ended)	7.7 mW	7.6 mW	79 μW
LIS2L02AL accelerometer	2.4 mW	–	–
ZMD31050 ASIC	7.5 mW	–	–
Voltage regulator (Differential)	0.13 mW	0.01 μW	0.01 μW
BDI strain transducer (350 Ω)	25.7 mW	–	–
Total: acceleration monitoring	79.4 mW	8.5 mW	132 μW
Total: strain monitoring	106.3 mW	8.5 mW	132 μW
Total: strain and acceleration	115.3 mW	8.5 mW	132 μW

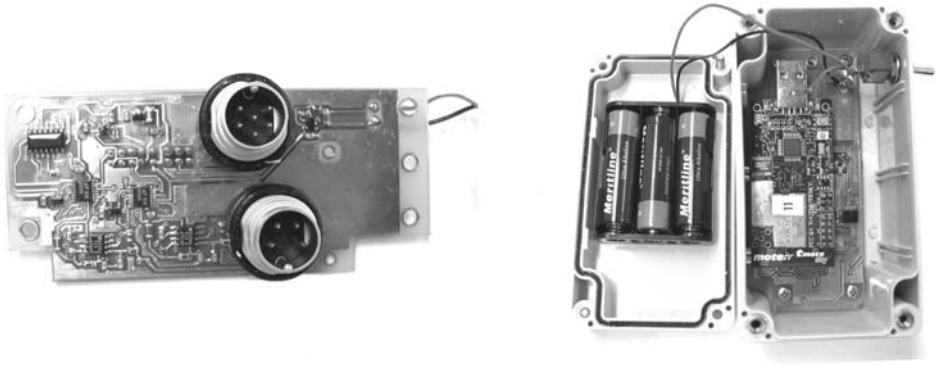

Figure 4. *Prototype signal conditioning board and assembled wireless sensor node.*

activity, the hardware can be placed in a low-power sleep mode to conserve power resources. In this state, either the voltage supply to the circuitry is switched off or the integrated circuit is set to function in a low-power state, if available. Since the PGA, programmable offset voltage references, and differential signal conditioning ASIC all feature non-volatile memory, the power to the sensors and signal conditioning can be cycled without having to reconfigure the signal conditioning settings. Furthermore, this allows the sensors and signal conditioning to be powered only during active sampling, to enable optimized power conservation during installation, in-network configuration, and network diagnostic periods.

In a long-term wireless sensor network deployment, a duty-cycle approach to sampling is generally preferred to reduce power consumption for extending the life of the battery resources and maintaining a manageable database of measurements. In order to maintain the proper regulation of the 3 V sensor excitation to ensure the integrity of the sensitivity for accurate measurements, the sensor nodes require a power supply providing at least 3.1 V. In the current prototype, three AA batteries with 2650 mAh capacity are used to power the wireless nodes, thereby providing a supply voltage of 4.2 V at full charge and utilizing about 90% of the battery resources before discharging below the operational voltage required by the nodes. Consequently, the ~2385 mAh effective capacity results in a continuous monitoring service life, as dictated by the battery resources, of ~68 h, or 2.8 days. Conversely, if a duty-cycle approach is implemented in which the sensor node only participates in active sampling for 1 min each hour, or 24 min per day, the service life is extended to 32 days. Consequently, an effective long-term structural health monitoring deployment will balance the requirements of the monitoring approach with the battery resources and acceptable service life of the instrumentation.

Several issues in power conservation were identified after the development of the prototype sensor nodes. First, the circuit does not provide a means to disrupt power to the voltage references used to offset the single-ended measurements, which each require 3.63 mW. Since these devices are non-volatile, supply could be disrupted to reduce power consumption during inactivity. Additional devices, such as the ADC reference and the PGA reference, could be isolated from the supply during inactivity for an additional reduction of 0.54 mW. Additionally, in deployments using low-voltage power supplies, such as batteries, the main voltage regulator can be removed to reduce idle consumption by an additional 0.56 mW. Implementation of these revisions in the board design will reduce idle power consumption to 132 μW and significantly increase the long-term duty-cycled service life of the nodes. For active sampling at a rate of 1 min per hour, the estimated service life would be extended to 160 days.

PERFORMANCE VALIDATION

Thorough laboratory validation tests, as well as field deployments, have been undertaken to evaluate the performance of the developed wireless bridge monitoring hardware platform as well as the sampling routine and radio transmission protocol. The scope of laboratory testing included spectral verification of accelerometer sensors, time synchronization verification of independent nodes, investigation of data success rates, and multi-axis modal analysis of a laboratory-scale bridge model. A large-scale high-rate field deployment on a single-span bridge served to further verify the system performance in a real-world setting.

Laboratory Testing

A Polytec scanning vibrometer was used to verify the acceleration spectra recorded by the wireless sensor nodes due to sinusoidal and sine-sweep inputs from a small shaker (Figure 5). A sequence of small amplitude tests was performed over a range of excitation frequencies across the measurement bandwidth. Comparisons between the spectra obtained by the vibrometer and the wireless accelerometer yield excellent correlation in terms of both the signal amplitude and frequency. Consequent to this comparison with state-of-the-art instrumentation benchmark measurements, the transfer function of the signal conditioning on the wireless node as well as the accuracy of the sampling clock are reasonably validated.

Field Deployment

A large-scale network consisting of 40 channels of sensor measurements acquired through 20 remote wireless transceiver nodes was deployed on an integral abutment, single-span bridge in St. Lawrence County, NY (Figure 6). The bridge is a 17.07 m (56 ft) span reinforced concrete deck on four steel girders spaced 2.74 m (9 ft) center-to-center. Both quasi-static, similar to load-rating protocol, and dynamic monitoring of the bridge was conducted using a total of 29 accelerometers and 11 strain transducers. LIS2L02AL MEMS Accelerometers were selected for low-noise, low-power vibration monitoring and were potted in an external sensor housing for direct placement on the structure. BDI Intelliducers, manufactured by Bridge Diagnostics Incorporated, were utilized for strain monitoring as these sensors feature a 3 inch gauge length, can be redeployed, and are currently used by several transportation agencies to perform in-service load ratings.

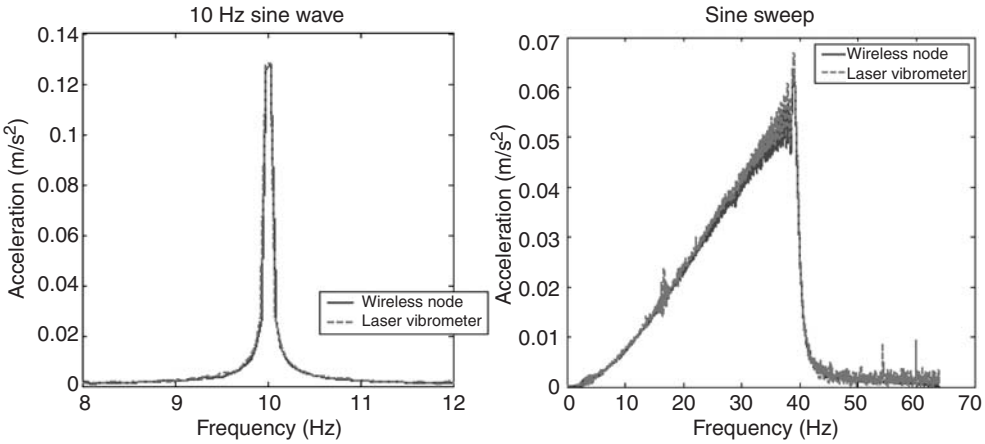

Figure 5. *Acceleration spectra comparison with laser vibrometer.*

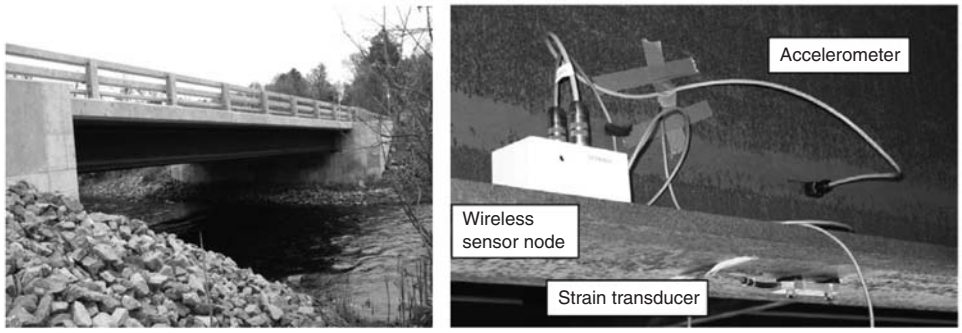

(a) View of wright road bridge (b) Typical sensor node installation

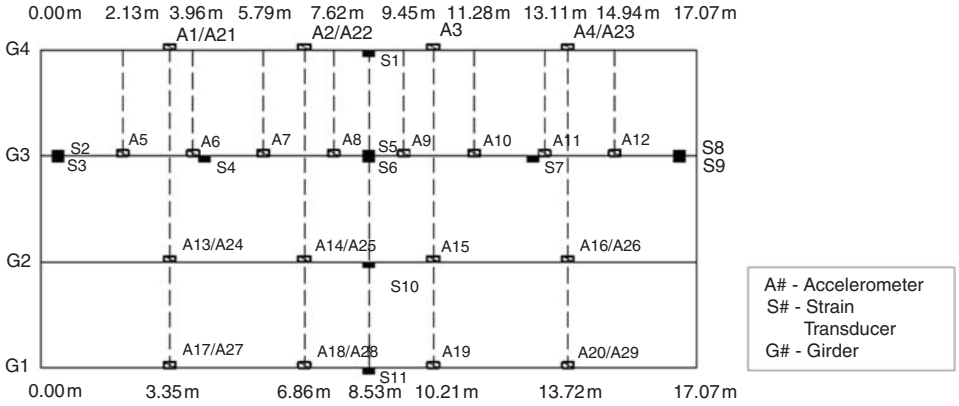

(c) Accelerometer and strain instrumentation plan

Figure 6. *Wright road bridge field deployment.*

Only ambient loading from vehicular traffic was provided for structural excitation. Each channel of sensor data was over-sampled at 512 Hz, passed through the default 56th-order digital low-pass filter, and decimated to an effective sampling rate of 128 Hz for real-time transmission to the host computer. This network configuration and sampling rate resulted in a transmission overhead in the range of 97–126 kbps depending on the initial packet success and retransmission rates.

The average packet success rate across all of the sensor nodes over 10 186 second test cycles was 99.91%, with 92% of the nodes reporting 100% packet delivery success. The minimum packet success rate over these tests was 98.0% (Figure 7). The small loss of data has been attributed to a software bug identified in the portion of the code responsible for transmitting any packets remaining in the transmission queue after completion of sampling. It is anticipated that correction of the software section responsible for transmitting

packets remaining in the queue will result in complete data sets; however at the current level of packet success over the sampling time, system identification analysis suffered from no noticeable or adverse distortion.

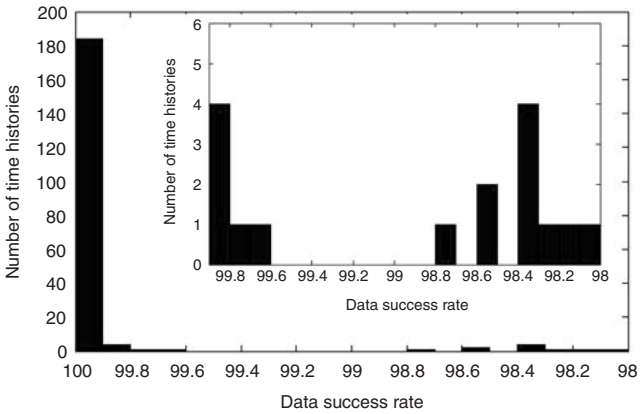

Figure 7. *Histogram of packet success rates over field deployment testing.*

This degree of transmission reliability at the high-data throughput rate attained in this testing reveals that wireless sensor networks are currently capable of performing large-scale structural health monitoring tasks with real-time transmission.

Integral abutment bridges are unique in that the primary longitudinal members, or girders, are cast integrally with the abutments rather than supported by bearings. Consequently, bridges with this design tend to exhibit stiffer behavior than designs of similar span length and, as a result, experience lower amplitude vibrations. Therefore, field deployment of an instrumentation system designed to measure the response from the wide spectrum of bridge designs can advantageously be tested on a single-span integral abutment bridge to provide a baseline 'worst-case' scenario from a signal-to-noise perspective. Throughout the deployment, local accelerations on the bridge generally produced peaks ranging from only around 2 mg to up to 10 mg, though were well-captured in the sensor time histories and frequency spectra (Figure 8).

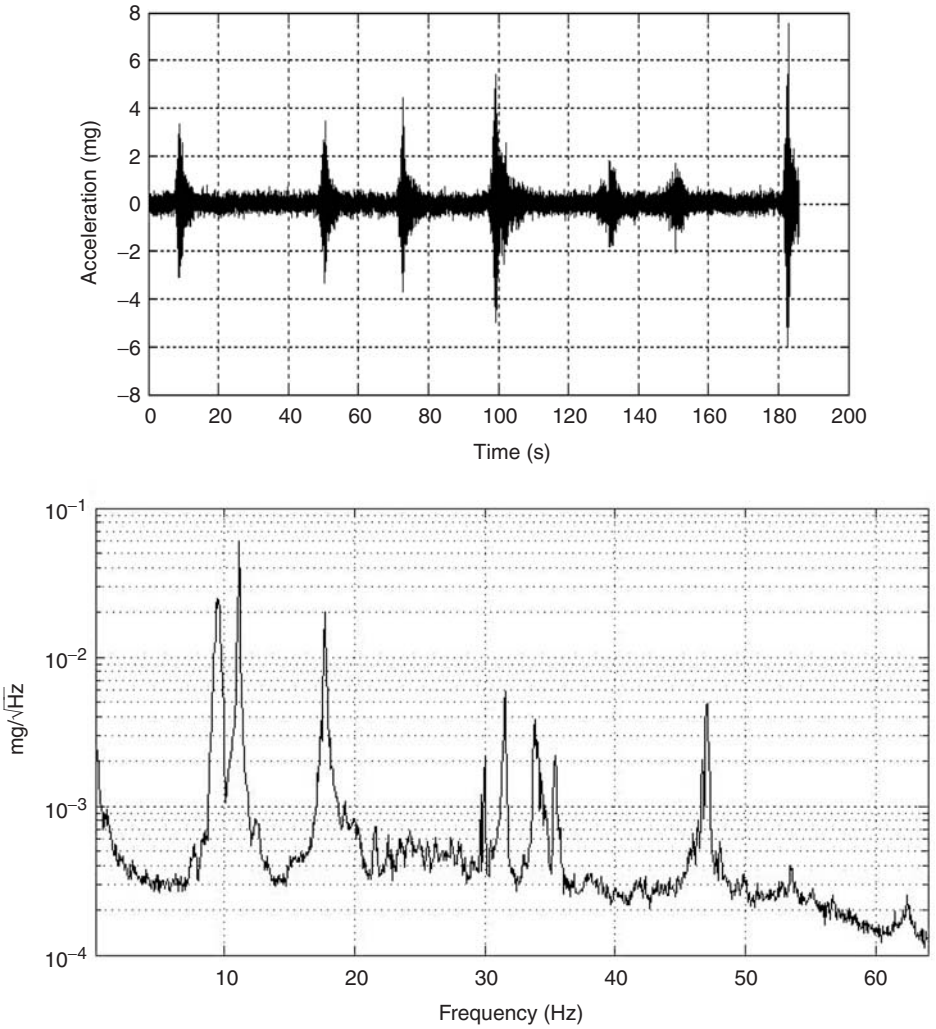

Figure 8. *Typical time history and average normalized power spectral density from 20 vertical accelerometers over a 186 s sampling duration.*

A significant percentage of damage detection algorithms proposed for the analysis of the dynamic response of civil structures rely on derivation of in-service mode shapes. To produce accurate mode shapes, not only do the modal frequencies need to be well represented in the frequency spectra, but the nodes must preserve reasonable time synchronization in order to maintain phase relationships. Furthermore, the phase relationship is hardest to maintain for high-frequency modes; the period of the signal, and hence the time synchronization tolerance, is relative to the frequency. In this study, mode shapes were derived from the 20 vertical acceleration measurements using the classical peak peaking method employed through Fourier analysis as well as stochastic sub-space identification (SSI) to reveal the 4th and 5th modes which were not excited well by traffic loading (Figure 9). These mode shapes are consistent with those of a plate with parallel fixed ends, and correlate well in terms of frequency and shape with finite element analysis from a model constructed from as-built drawings. To the authors' knowledge, derivation of nine experimental mode shapes with frequencies ranging up to 47 Hz is the highest order mode development from a real-time wireless sensor network. This analysis is afforded only through sufficient time synchronization coupled with the high nodal density facilitated by the radio transmission protocol.

Deployment of strain transducers alongside the accelerometers demonstrated the versatility of the sensor nodes and capability of the system to be deployed as an alternative to cable-based systems currently used for load ratings. The layout of the strain transducers (Figure 6(c)) provides typical placement to measure bridge properties of interest, such as neutral axis locations, section modulus, and distribution factors. Despite that the applied loads from the passenger vehicle are significantly lower than typically imposed during a load rating, strain profiles resulting from passenger vehicle traffic were well represented by the 15-bit ADC provided in the differential signal conditioning ASIC. The development of bending strain in the girders during a crawl-speed pass of a large sports utility vehicle was well captured (Figure 10). The localized tension spike recorded at the top of the girder at the mid-span occurs when the vehicle wheel is directly overhead the sensor location. Strain profiles were found to be

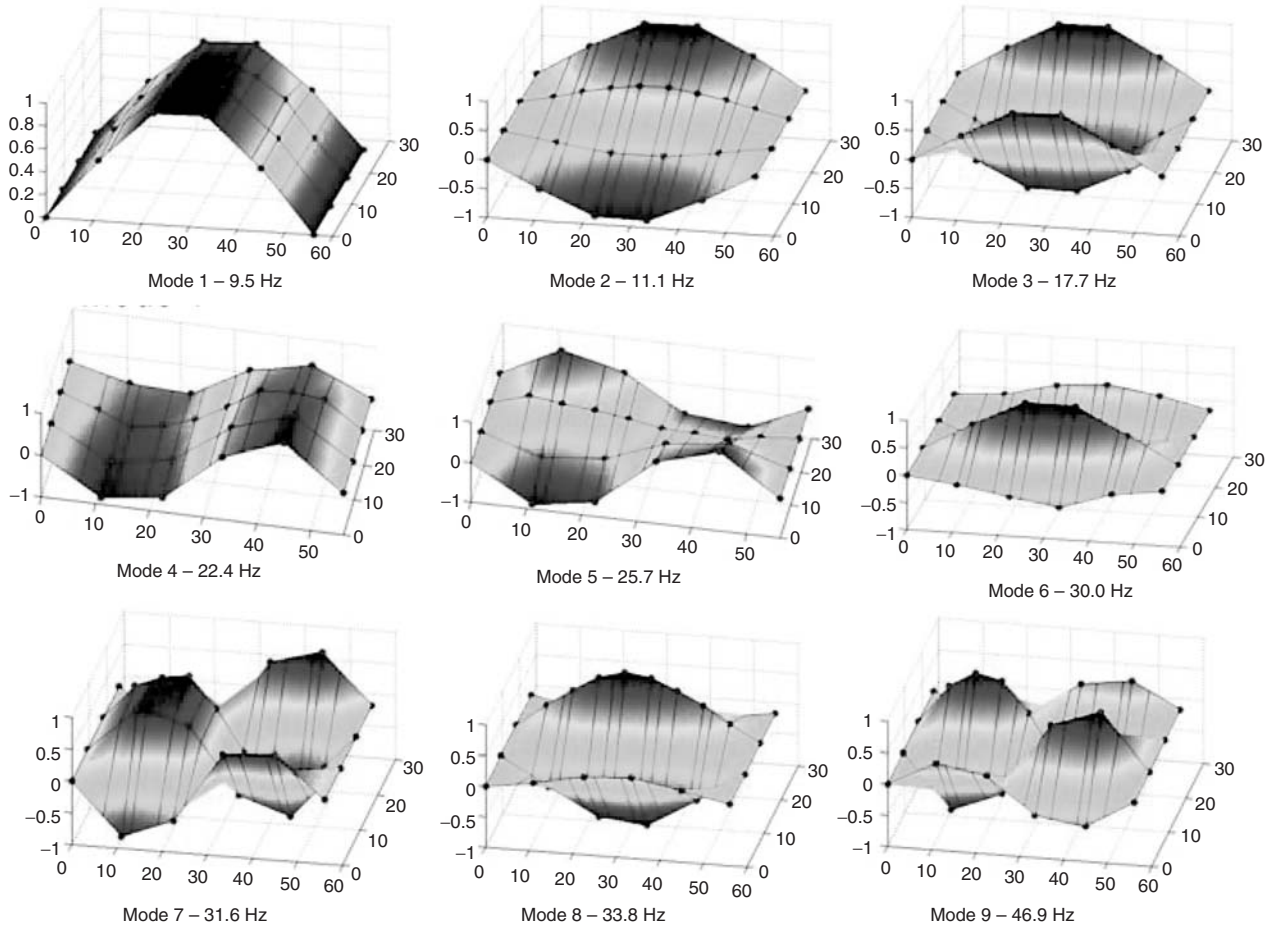

Figure 9. *Mode shapes derived from experimental measurements.*

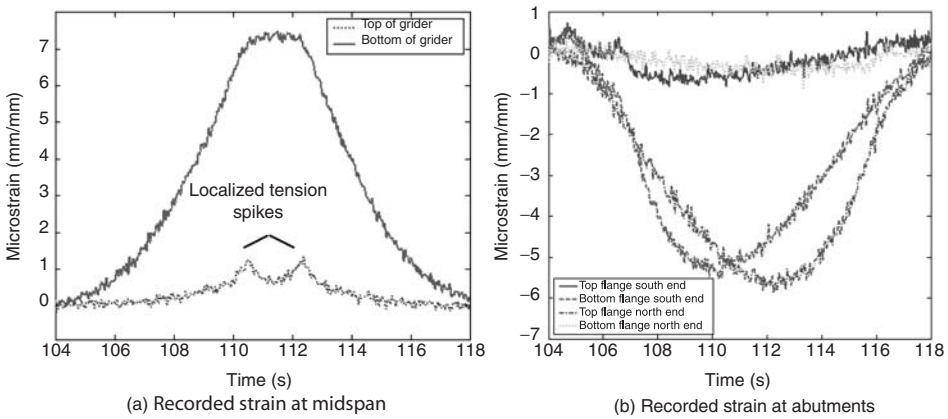

Figure 10. *Representative strain transducer response.*

consistent with vehicle loading patterns, composite action of the deck and girders was verified, and the calculated neutral axis locations were found to correlate well with theoretical calculations.

CONCLUSION AND DISCUSSION

A WSS for high-rate real-time sampling from large, distributed sensor arrays has been developed in the LIITT at Clarkson University. The system is multi-functional in that it provides a low-power platform for the concurrent deployment of accelerometers, strain transducers, and temperature sensors. The hybrid sensing capabilities of these nodes satisfies the immediate requirements for economic, low-maintenance load ratings and short-term dynamic vibration measurements, in addition to providing the hardware functionality for development of a long-term continuous bridge monitoring system.

The wireless sensor network presented in this article is unique in that it has enabled the simultaneous acquisition of up to 40 channels of sensor data across 20 sensor nodes at high sampling rates in real-time without the data loss typically associated with wireless sensor networks. Extensive laboratory development has produced a robust network transmission protocol capable of sustaining a large number of nodes with high data throughput in real-time. Field deployments have verified the ability of the system to capture natural frequencies and accurately construct mode shapes from even a relatively stiff highway bridge, as well as record the localized strain profiles induced by vehicular traffic. The ability of this wireless sensor network to replicate the performance of cable-based deployments, in terms of the number of sensors and sampling rates, and ability to produce concise analysis results, signals a breakthrough in wireless structural health monitoring. Such emerging technology appears to be presently capable of performing the bridge monitoring tasks that have been highly proposed and promised, though seldom demonstrated, since the advent of low-cost wireless sensing technology.

ACKNOWLEDGMENTS

This research has been funded by the New York State Energy Research and Development Authority (NYSERDA), in collaboration with the St Lawrence Highway Department, and the New York State Department of Transportation (NYSDOT). The authors would also like to acknowledge Dr Ratneshwar Jha and graduate students Michael Gangone, Dan Nyanjom, Michael Fuchs, and Kevin Cross for their assistance in the study and field deployment.

REFERENCES

Chase, S.B. 2005. "The Role of Sensing and Measurement in Achieving FHWA's Strategic Vision for Highway Infrastructure," In: Ansari, F. (ed.), *Sensing Issues in Civil Structural Health Monitoring*, pp. 23–32, Springer, Netherlands.

Griffiths, D.J. 2006. *Introduction to Electrodynamics*, 3rd edn, p. 576, Prentice-Hall, New Delhi, India.

Kata, M. and Shimada, S. 1986. "Vibration of PC Bridge during Failure Process," *Journal of Structural Engineering*, 112(7):1692–1703.

Lynch, J.P. and Loh, K.J. 2006. "A Summary Review of Wireless Sensors and Sensor Networks for Structural Health Monitoring," *The Shock and Vibration Digest*, 38(2): 91–128.

Lynch, J.P., Sundararajan, A., Law, K.H., Kiremidjian, A.S. and Carryer, E. 2004. "Embedding Damage Detection Algorithms in a Wireless Sensing Unit for Operational Power Efficiency," *Smart Materials and Structures*, 13(4):800–810.

Lynch, J.P., Wang, Y., Loh, K.J., Yi, J.-H. and Yun, C.-B. 2006. "Performance Monitoring of the Geumdang Bridge using a Dense Network of High-resolution Wireless Sensors," *Smart Materials and Structures*, 15(6):1561–1575.

Moore, M., Phares, B., Graybeal, B., Rolander, D. and Washer, G. 2001. Reliability of Visual Inspection for Highway Bridges, Volume 1: Final Report. Federal Highway Administration. FHWA-RD-01-020.

Paek, J., Jang, O.G.K.-Y, Nishimura, D., Govindan, R., Caffrey, J., Wahbeh, M. and Masri, S. 2006. "A Programmable Wireless Sensing System for Structural Monitoring," In: *4th*

World Conference on Structural Control and Monitoring, San Diego, CA.

Pakzad, S.N., Fenves, G.L., Kim, S. and Culler, D.E. 2008. "Design and Implementation of Scalable Wireless Sensor Network for Structural Monitoring," *Journal of Infrastructure Systems*, 14:89–101.

Wenzel, H. and Pichler, D. 2005. *Ambient Vibration Monitoring*, John Wiley & Sons Ltd, West Sussex, England.

Whelan, M.J., Fuchs, M.P. and Janoyan, K.D. 2008. "Large Scale Remote Sensing for Environmental Monitoring of Infrastructure," *Journal of Environmental Monitoring*, 10:812–816.